Properties, Performance and Stability of Iridium-Coated Water Oxidation Electrodes based on Anodized Titanium Felts

André Hofer,[a] Sebastian Bochmann,[a] and Julien Bachmann[a,b]

1 Electrochemical performance

1.1 Electrochemical impedance spectroscopy (EIS)

The values for the uncompensated resistance R_u, the behavior of the full porous matrix as a dielectric (R_p and C_p), the charge transfer resistance R_{ct} and double layer capacitance C_{dl} of the electrochemical impedance spectroscopy (EIS) data are calculated by fitting the measured data using the equivalent circuit model shown in Figure S1.

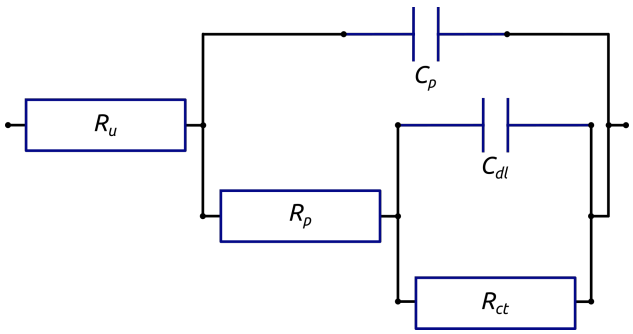

Fig. S1 Equivalent circuit model used for electrochemical performance characterizations by fitting EIS data.

1.2 Roughness factor *rf*

1.2.1 Geometry

The full surface area and thus the roughness factor are calculated based on the following geometric parameters: pore length l of 1 μm, pore inner diameter d and pore wall thickness w, based on the approximation of a hexagonal arrangement of the titania nanotubes illustrated in Figure S2. Using Equation 1 yields the results of the roughness factor summarized with the geometric parameters in Table S1. The length a of the triangular unit shown is the sum of the pore inner diameter d and two times the pore wall thickness w. The area of the triangle corresponds to a half tube. This defines the amount of tubes covering a unit area (1 cm^2). Finally, the roughness factor rf_{geo} is calculated from the product of a single tube's inner shell surface area and the amount of tubes.

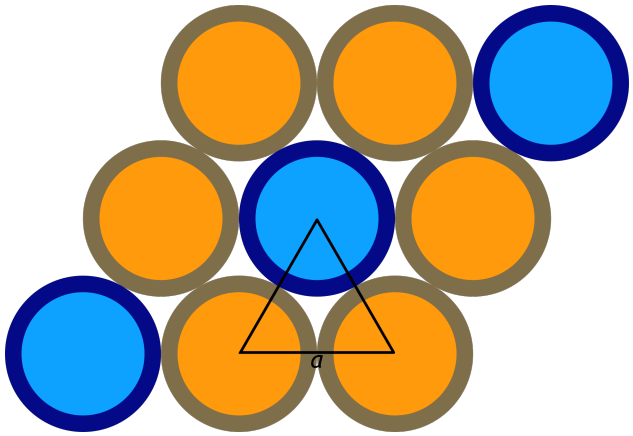

Fig. S2 Hexagonal arrangement of titania tubes for geometric roughness factor calculations.

[a] *Friedrich-Alexander University of Erlangen-Nürnberg, Department of Chemistry and Pharmacy, Chemistry of Thin Film Materials, IZNF / Cauerstr. 3, 91058 Erlangen, Germany; E-mail: julien.bachmann@fau.de*
[b] *Saint-Petersburg State University, Institute of Chemistry, Universitetskii pr. 26, 198504 St. Petersburg, Russia*

$$rf_{geo} = \frac{1\ cm^2}{2(\frac{a^2\sqrt{3}}{4})} \times d\pi l \tag{1}$$

Table S1 Summary of geometric parameters and resulting roughness factor *rf*.

sample	inner diameter d	wall thickness w	rf
12%, 2h	50	36	11
12%, 4h	40	16	27
50%, 2h	40	23	19
50%, 4h	54	25	15
100%, 2h	85	7	31
100%, 4h	46	19	24

1.2.2 Cyclic voltammetry

Cyclic voltammerty (CV) measurements are frequently utilized for electrochemical active surface area (ECSA) characterizations of noble metal catalyst electrodes.[1–4] The intensity (area) of the proton reductive adsorption peak in CV measurements is integrated at various scan rates (200, 100, 50, 25, 10 mV s^{-1}). The analysis relies on the fact that the integrated charge q depends on the scan rate v, which can be seen by plotting the charge q vs. scan rate v (Figure S3). The higher the scan rate, the lower is the integrated charge for the proton reductive adsorption (because if the integration over time). Consequently, the entire charge can be divided into two contributions: (i) the 'inner' caused by the existence of less accessible surface area generated in the pores/tubes and (ii) the 'outer' easy accessible surface sites (baseline). Our electrodes are anodized Ti fibers resulting in a surface enlargement by titanium dioxide nanotubes on every single fiber. The newly created surface area is predominantly on the inner wall of the titania tubes and thus belongs to the 'inner' (less accessible) surface. Increase of the scan rate leads to a decrease in the total charge due to exclusion of less accessible surface sites where diffusion to the surface becomes the rate-determining step. Therefore, q should be linearly dependent on the diffusion time and thus $q(v) \sim v^{-0.5}$. Extrapolation to $v^{-0.5} = 0$ gives the extreme value of an infinitely fast scan rate ($v = \infty$) and therefore the capacitance of the easily accessible 'outer' surface area, and thus the baseline capacity of the system. On the other extreme, decreasing the scan rate leads to an increase in the measured capacitive charge because the 'inner' surface area requires longer diffusion times. Therefore, it is expected that $q(v)^{-1} \sim v^{0.5}$. Extrapolation of $v^{0.5} = 0$ gives the extreme value of an infinity slow scan rate ($v = 0$) and therefore the total capacitance.

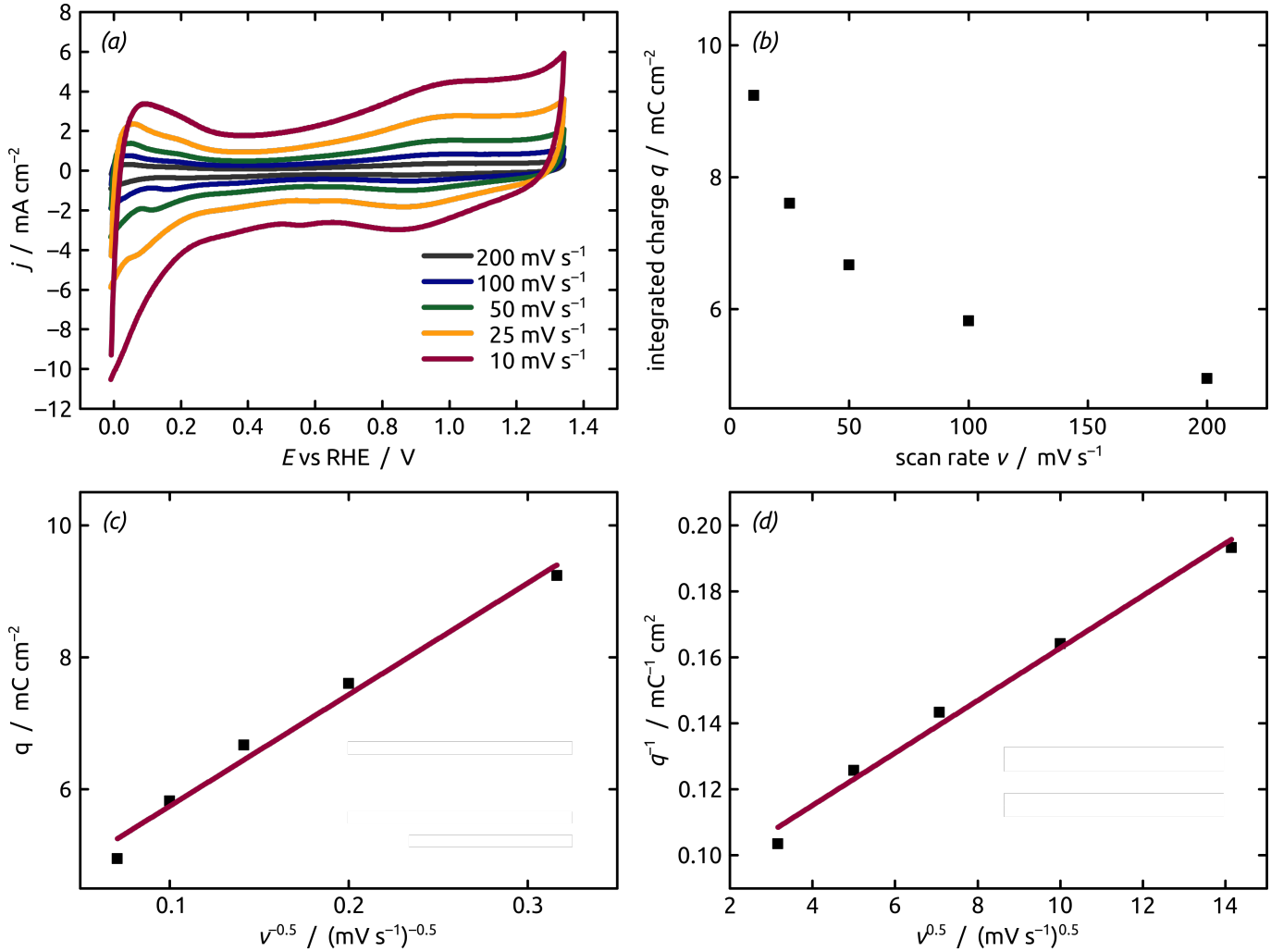

Fig. S3 *(a)* CVs with varied scan rates ν, *(b)* integrated charge q vs. the scan rate, *(c)* linear fit of integrated charge vs $\nu^{-0.5}$ yielding a intercept of 4.15 ± 0.26 mC cm^{-2} ($R^2 = 0.98$), *(d)* linear fit of inverse charge vs. $\nu^{0.5}$ yielding in a intercept of $0.09 \pm 4{\times}10^{-3}$ mC^{-1} cm^2 ($R^2 = 0.98$).

For the electrocatalytically active surface area (ECSA), the capacity q_H determined for the integrated proton reduction peak is subtracted from the extrapolated q_{outer} ($\nu = \infty$) as a baseline correction. Subsequently, the averaged q ("baseline" corrected capacities at different scan rates) is divided by the surface coverage factor θ for adsorbed hydrogen for polycrystalline Ir ($\theta = 0.65$)[4] multiplied with the charge of a monolayer of hydrogen on polycrystalline Ir ($q_{ML,s} = 218\ \mu$C cm^{-2})[4] to yield the electrocatalytically active surface area. Finally, the roughness factor rf_{CV} is the quotient of the calculated ECSA and the macroscopic surface area A_{macro}.

$$rf_{CV} = \frac{ECSA}{A_{macro}} = \frac{\frac{q_H}{\theta \times q_{ML,s}}}{A_{macro}} \tag{2}$$

1.2.3 Electrochemical impedance spectroscopy (EIS)

Electrochemical impedance spectroscopy (EIS) performed at the hydrogen adsorption potential is utilized to determine C_{ads}, the capacitance of the hydrogen adsorption reaction, which is equal to the value q_H determined above via CV measurements.

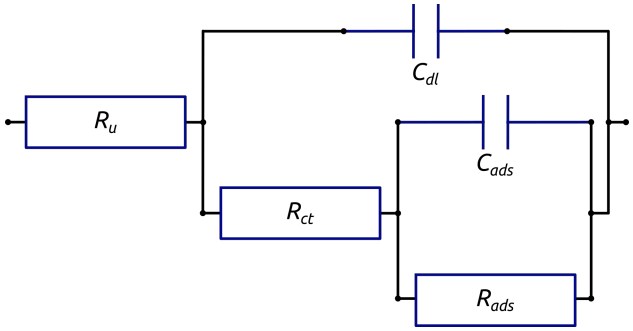

Fig. S4 Equivalent circuit model[5] used for real surface area characterizations by fitting EIS data.

2 Stability

2.1 Electrochemical stability

Table S2 Initial and final maximum current densities j_{max} at an applied overpotential of $\eta = 0.44$V in linear sweep voltammetry (LSV) measurements with a scan rate of 2 mV s^{-1} in a stirred 1 M H_2SO_4 aqueous solution at 60 °C.

sample	initial j_{max} / mA cm^2	final j_{max} / mA cm^2	ratio / %
12%, 2 h	75.2 ± 3.5	76.6 ± 4.1	102
12%, 4 h	66.1 ± 2.0	69.8 ± 3.6	106
50%, 2 h	52.0 ± 4.2	41.7 ± 4.4	80
50%, 4 h	47.0 ± 3.5	36.2 ± 7.4	77
100%, 2 h	33.4 ± 7.9	14.2 ± 9.4	43
100%, 4 h	30.3 ± 14	19.2 ± 13	63

2.2 Chemical stability

Table S3 Energy-dispersive X-ray spectroscopy (EDS) analysis for initial Ir and Ti content and Ir/Ti ratio determination.

sample	$Ir_{initial}$ / at%	$Ti_{initial}$ / at%	Ir/Ti ratio / %
12%, 2 h	9.2 ± 2.2	25.5 ± 4.3	36
12%, 4 h	7.5 ± 0.8	31.6 ± 1.8	24
50%, 2 h	3.1 ± 0.7	35.1 ± 3.2	9
50%, 4 h	3.9 ± 0.6	37.2 ± 6.4	10
100%, 2 h	3.1 ± 0.1	32.1 ± 1.7	10
100%, 4 h	1.9 ± 0.2	29.6 ± 2.0	6

Table S4 Energy-dispersive X-ray spectroscopy (EDS) analysis for initial and final (after complete electrochemical characterization) Ir content determination.

sample	$Ir_{initial}$ / at%	Ir_{final} / at%	ratio / %
12%, 2 h	9.2 ± 2.2	5.0 ± 1.6	55
12%, 4 h	7.5 ± 0.8	2.5 ± 1.4	33
50%, 2 h	3.1 ± 0.7	2.0 ± 0.1	64
50%, 4 h	3.9 ± 0.6	2.3 ± 0.5	60
100%, 2 h	3.1 ± 0.1	0.6 ± 0.3	21
100%, 4 h	1.9 ± 0.2	0.5 ± 0.3	26

2.3 Physical stability

The physical stability is characterized by scanning electron microscopy micrographs (Figure S5 and S6) and quantified based the following four criteria:

(i) the generation of open pores or free standing tubes

(ii) a homogeneous nanostructured surface on all fibers of the Ti substrate

(iii) a titanium dioxide structure with no cracks, damages or peeling off

(iv) an enhanced surface area on the Ti substrate with a good overall optical impression

Table S5 Summary of the four categories used to analyze the physical stability by evaluate SEM micrographs, ● indicates a point for the certain category, whereas ❍ indicates the criterion is not fulfilled.

sample	status	(i) tubes	(ii) homogeneous	(iii) no peeling off	(iv) overall	Σ
12%, 2 h	initial	●	●	●	❍	3
	final	●	●	●	❍	3
12%, 4 h	initial	●	●	●	●	4
	final	●	❍	❍	❍	1
50%, 2 h	initial	●	❍	●	❍	2
	final	●	❍	❍	❍	1
50%, 4 h	initial	●	●	●	❍	3
	final	●	●	❍	❍	2
100%, 2 h	initial	●	❍	❍	❍	1
	final	●	❍	❍	❍	1
100%, 4 h	initial	●	❍	●	❍	2
	final	●	❍	❍	❍	1

The changes of the surface and thus the physical stability is calculated by dividing the final by the initial score, multiplied by a normalization factor (the initial score divided by the maximum score of 4, Equation 3). The final value for the physical stability is presented in Table S6.

$$stb_{phy} = \frac{\text{final score}}{\text{initial score}} \times \frac{\text{initial score}}{4} \tag{3}$$

Table S6 Summary of initial and final score, the normalization factor (initial divided by 4) and the resulting number for the physical stability.

sample	initial	final	factor	%
12%, 2h	3	3	0.75	75
12%, 4h	4	1	1.00	25
50%, 2h	2	1	0.50	25
50%, 4h	3	2	0.75	50
100%, 2h	1	1	0.25	25
100%, 4h	3	1	0.75	25

References

1 S. Ardizzone, G. Fregonara and S. Trasatti, *Electrochim. Acta*, 1990, **35**, 263 – 267.

2 S. Trasatti and O. Petrii, *J. Electroanal. Chem.*, 1992, **327**, 353 – 376.

3 R. F. Savinell, *J. Electrochem. Soc.*, 1990, **137**, 489.

4 M. Łukaszewski, M. Soszko and A. Czerwińsk, *Int. J. Electrochem. Sci.*, 2016, **11**, 4442–4469.

5 S. Watzele and A. S. Bandarenka, *Electroanalysis*, 2016, **28**, 2394–2399.

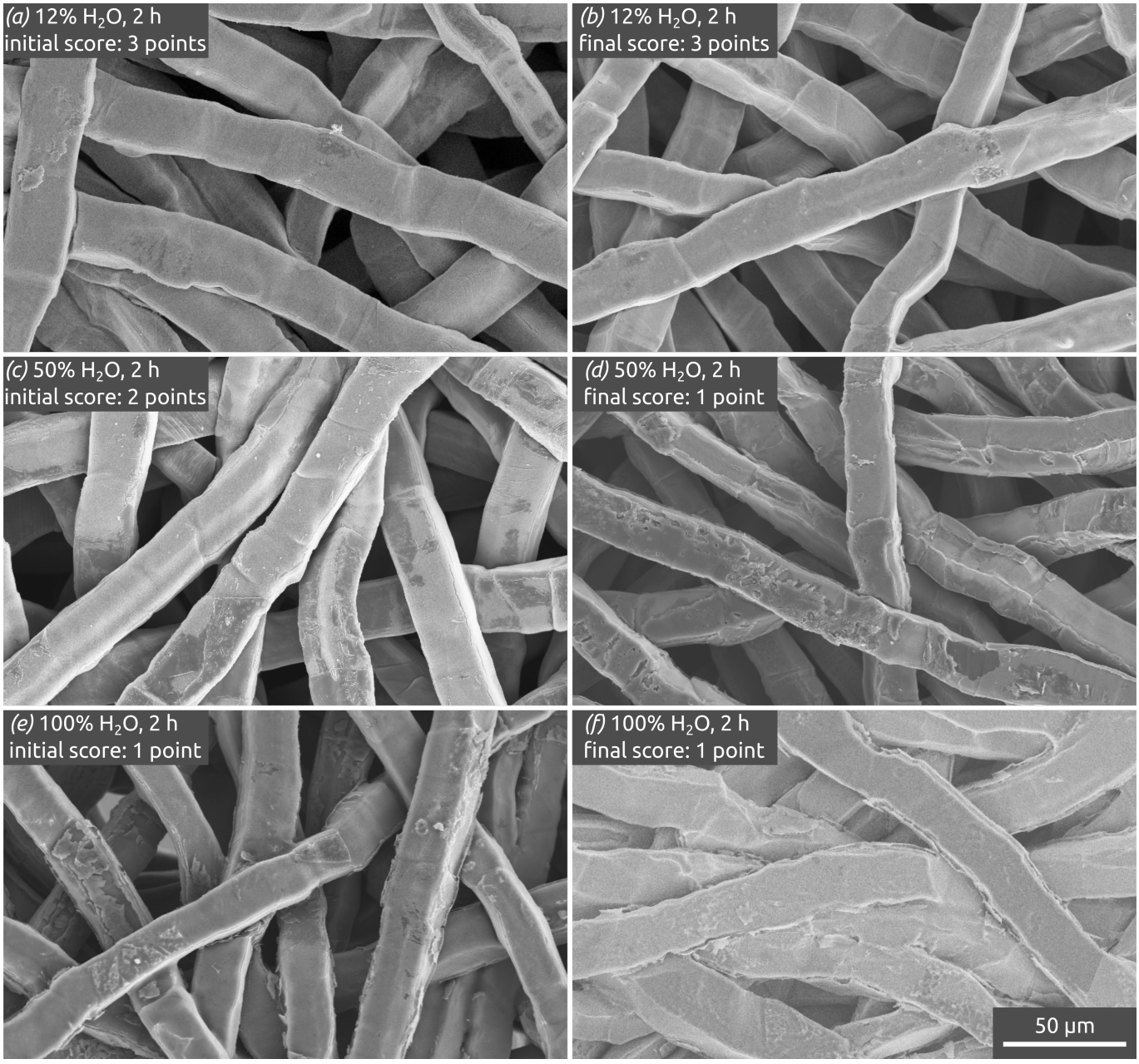

Fig. S5 Characterization of the titanium felt electrodes obtained after anodization and Ir coating before *(a), (c), (e)* and after electrochemical measurements in stirred 1 M H_2SO_4 aqueous solution at 60°C *(b), (d), (f)*. Titanium was anodized for 2 h in glycerol-based electrolytes with 12% water under 40 V *(a)/(b)*, 50% water under 20 V *(c)/(d)* and 100% water under 20 V *(e)/(f)*, yielding a tube inner diameter increasing from 40 nm to 50 nm and 85 nm, whereas all feature the same pore length of approx. 1 μm.

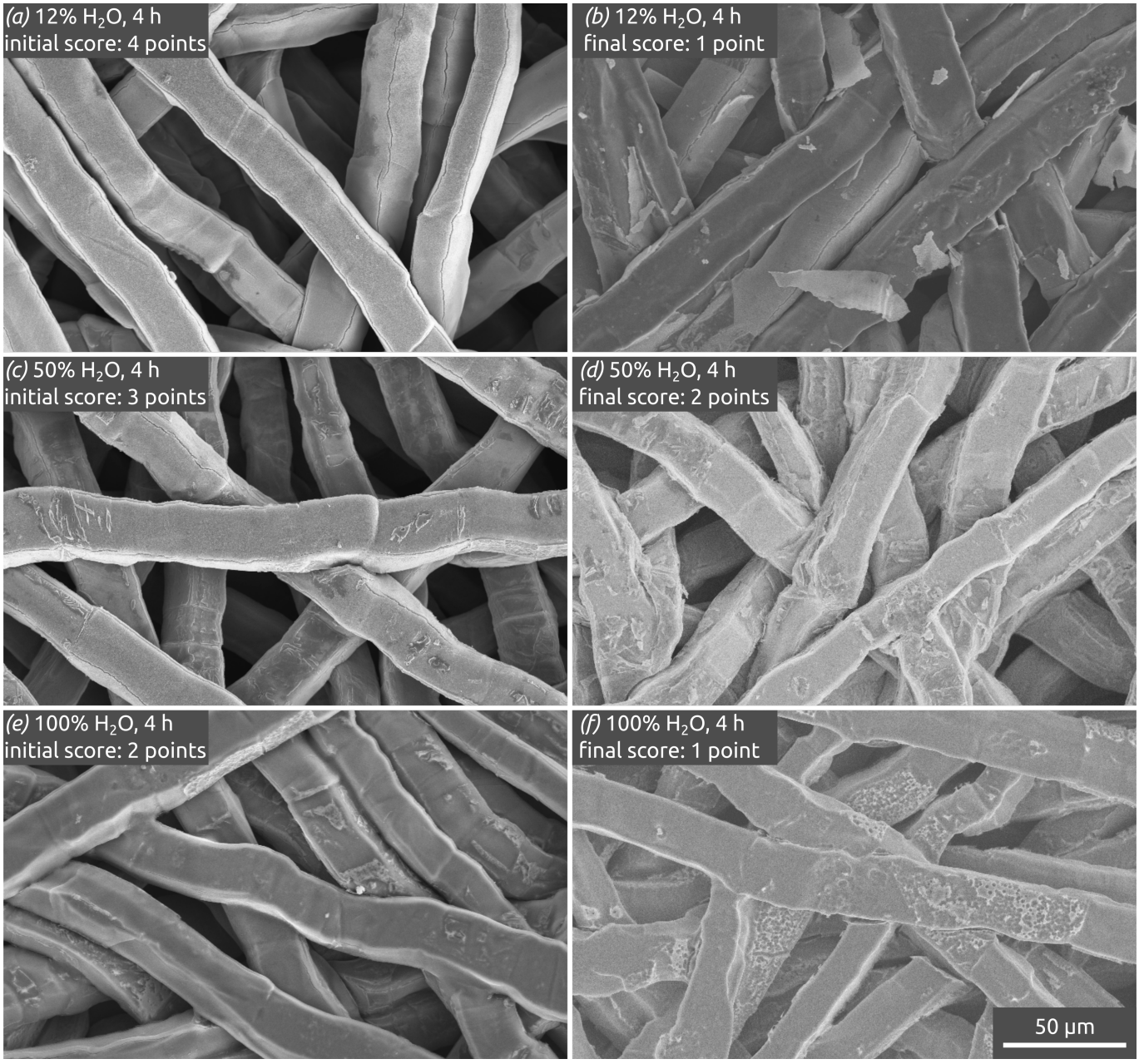

Fig. S6 Characterization of the titanium felt electrodes obtained after anodization and Ir coating before *(a), (c), (e)* and after electrochemical measurements in stirred 1 M H_2SO_4 aqueous solution at 60°C *(b), (d), (f)*. Titanium was anodized for 4 h in glycerol-based electrolytes with 12% water under 40 V *(a)/(b)*, 50% water under 20 V *(c)/(d)* and 100% water under 20 V *(e)/(f)*, yielding a tube inner diameter increasing from 40 nm to 50 nm and 85 nm and all feature the same pore length of approx. 1 μm.